EBioMedicine 41 (2019) 320–332

Contents lists available at ScienceDirect

EBioMedicine

journal homepage: www.ebiomedicine.com

EBioMedicine
Published by THE LANCET

POH1 contributes to hyperactivation of TGF-β signaling and facilitates hepatocellular carcinoma metastasis through deubiquitinating TGF-β receptors and caveolin-1

Boshi Wang [a,1], Xiaoli Xu [b,1], Zhaojuan Yang [a,1], Li Zhang [a], Yun Liu [a], Aihui Ma [a], Guiqin Xu [a], Ming Tang [a], Tiantian Jing [a], Lin Wu [a], Yongzhong Liu [a,*]

[a] State Key Laboratory of Oncogenes and Related Genes, Shanghai Cancer Institute, Renji Hospital, Shanghai Jiao Tong University School of Medicine, Shanghai 200032, China
[b] State Key Laboratory of Oncogenes and Related Genes, Renji Hospital, School of Biomedical Engineering, Shanghai Jiao Tong University, Shanghai 200240, China

ARTICLE INFO

Article history:
Received 9 October 2018
Received in revised form 30 January 2019
Accepted 30 January 2019
Available online 7 February 2019

Keywords:
POH1
TGF-β signaling
TGF-β receptor
Hepatocellular carcinoma.

ABSTRACT

Background: Hyper-activation of TGF-β signaling is critically involved in progression of hepatocellular carcinoma (HCC). However, the events that contribute to the dysregulation of TGF-β pathway in HCC, especially at the post-translational level, are not well understood.
Methods: Associations of deubiquitinase POH1 with TGF-β signaling activity and the outcomes of HCC patients were examined by data mining of online HCC datasets, immunohistochemistry analyses using human HCC specimens, spearman correlation and survival analyses. The effects of POH1 on the ubiquitination and stability of the TGF-β receptors (TGFBR1 and TGFBR2) and the activation of downstream effectors were tested by western blotting. Primary mouse liver tissues from polyinosinic:polycytidylic acid (poly I:C)- treated Mx-Cre+, *poh1*$^{f/f}$ mice and control mice were used to detect the TGF-β receptors. The metastatic-related capabilities of HCC cells were studied *in vitro* and in mice.
Findings: Here we show that POH1 is a critical regulator of TGF-β signaling and promotes tumor metastasis. Integrative analyses of HCC subgroups classified with unsupervised transcriptome clustering of the TGF-β response, metastatic potential and outcomes, reveal that POH1 expression positively correlates with activities of TGF-β signaling in tumors and with malignant disease progression. Functionally, POH1 intensifies TGF-β signaling delivery and, as a consequence, promotes HCC cell metastatic properties both *in vitro* and *in vivo*. The expression of the TGF-β receptors was severely downregulated in POH1-deficient mouse hepatocytes. Mechanistically, POH1 deubiquitinates the TGF-β receptors and CAV1, therefore negatively regulates lysosome pathway-mediated turnover of TGF-β receptors.
Conclusion: Our study highlights the pathological significance of aberrantly expressed POH1 in TGF-β signaling hyperactivation and aggressive progression in HCC.

1. Introduction

Transforming growth factor β (TGF-β) acts as a promoter or a tumor suppressor of tumor progression depending on tumor types, stages and cellular contexts [1,2]. In liver tumorigenesis, most evidence indicates that TGF-β signaling contributes to tumor cell proliferation, metastasis and remodeling of the tumor microenvironment [3]. Notably, genetic manipulation and knockdown of the components of TGF-β signaling reveal that TGF-β greatly enhances liver tumorigenesis in mice [4–6]. Moreover, in human hepatocellular carcinoma (HCC) tissues, serum TGF-β levels and the activation of the intracellular downstream effectors are positively associated with poor outcomes of HCC patients [7,8]. Integrative transcriptome studies propose hyperactivation of TGF-β signaling as the main characteristic of HCC with aggressive behavior and poor prognosis [9,10]. Although hyper-activated TGF-β signaling has been known to facilitate HCC development and progression. However, the mechanisms underlying dysregulated TGF-β signaling in HCC remain elusive.

Deubiquitination is considered to play key roles in maintaining cellular homeostasis and proper functions. Numerous evidences suggest that dysfunction of deubiquitinating enzymes (DUBs) is responsible for multiple types of diseases including cancer [11–14]. Some DUBs are aberrantly expressed in HCCs and regulate the tumorigenesis and progression of HCC, such as OTUB1 [15], USP9X [16] and PPPDE1 [17].

* Corresponding author.
E-mail address: liuyzg@shsci.org (Y. Liu).
[1] These authors contribute equally to this work.

https://doi.org/10.1016/j.ebiom.2019.01.058

Research in context

Evidence before this study

Hyperactivation of TGF-β signaling is one of the main characteristics of hepatocellular carcinoma (HCC) with aggressive behavior and poor prognosis. Consistently, in liver tumorigenesis, TGF-β signaling contributes to HCC cell proliferation, metastasis and remodeling of the tumor microenvironment. POH1 is aberrantly expressed in multiple types of cancers and functions as a deubiquitinating enzyme that contributes to tumor growth and progression. However, the role for POH1 in the regulation of TGF-β signaling is still unrecognized.

Added value of this study

We categorized HCCs with the molecular classification based on the activities of TGF-β signaling, metastatic capability and clinical outcomes. POH1 hyperactivation is positively associated with the strength of TGF-β signaling, tumor metastasis as well as poor outcomes of HCC patients. Furthermore, the present study revealed a role for POH1 in deubiquitinating and stabilizing the TGF-β receptors, thereby promoting activation of TGF-β signaling and HCC metastasis.

Implications of all the available evidence

The present work proposes POH1-mediated regulation of TGF-β signaling as an event critical for HCC progression and suggests that POH1 may be a promising target for HCC treatment.

It has been known that the TGF-β receptors can be deubiquitinated and stabilized by USP4, USP15 and USP11 [18–20]. However, little is known about DUBs that can regulate the TGF-β signaling in the context of HCCs.

POH1/rpn11/PSMD14 is associated to 19S regulatory particle and serves as a deubiquitinating enzyme that regulates various biological processes and pathways, including proteasomal activity [21,22], aggresome clearance [23], DNA double strand breaks [24], embryonic stem cell differentiation [25] and cell survival [26]. POH1 belongs to the JAMM (JAB1/MPN+/MOV34) domain metalloprotease family of DUBs. Our previous study revealed that POH1 is aberrantly expressed in HCC tissues and promotes tumor development by deubiquitinating and stabilizing the transcription factor E2F1 [27]. Recently, emerging evidence demonstrated the deregulation and implication of POH1 in different types of malignancies, such as esophageal squamous cell carcinoma [28], myeloma [29], and breast cancer [30].

Given the importance of TGF-β signaling in tumor development and progression, we set out to interrogate key deubiquitination events underlying aberrant activation of TGF-β signaling in HCC. Through classification of HCC patients from independent cohorts, *in silico* screening of DUBs expression and functional analyses, we demonstrated that the dubiquitinase POH1 deubiqutinates and stabilizes the TGF-β receptors and thereby potentiates tumor metastasis. These findings therefore reveal a previously unrecognized role for POH1 in regulating TGF-β-related malignant progression in hepatocellular carcinoma.

2. Materials and methods

2.1. Classification of samples in datasets and gene set enrichment analysis

TCGA-LIHC gene expression matrix and clinical information were downloaded from UCSC Xena web site (https://xenabrowser.net/datapages/?cohort=TCGA%20Liver%20Cancer%20(LIHC)). Gene expression data of GSE14520 and GSE54236 datasets were downloaded from GEO database. Gene signatures was from Molecular Signatures Database (MSigDB) (http://software.broadinstitute.org/gsea/msigdb/index.jsp). Activity score of each gene signature in each sample was determined by single sample gene set enrichment analysis (ssGSEA, Gene Pattern module). Molecular classification was performed using R statistical packages version 3.5.1. Unsupervised clustering was achieved using k-means by the kmeans function in R package stats. Gap statistics was calculated to determine the optimal number of clusters. The signatures of Hoshida classes were derived from MSigDB. Nearest Template Prediction (NTP) analysis (Gene Pattern modules) was performed to classify samples into the published classes using the default parameters. TGF-β_activity_score was defined by the geometric mean of ssGSEA scores of the TGF-β positively regulated gene signatures KARLSSON_TGFB1_TARGETS_UP and COULOUARN_TEMPORAL_TGFB1_SIGNATURE_UP. The subpopulation specific genes were determined by a two-step algorithm Significance Analysis of Microarrays (SAM) followed by Prediction Analysis of Microarray (PAM) as described by Sadanandam, et al. [31]. The POH1 regulated genes were determined by our previously published genome-wide transcription profiles of HCC cell lines (GSE65210) overlapped with the genes correlated with POH1 expression in TCGA-LIHC dataset. Heatmaps were generated by ComplexHeatmap packages. Gene Set Enrichment Analysis (GSEA) was performed using the GSEA program provided by the Broad Institute (http://www.broadinstitute.org/gsea/index.jsp).

2.2. Cell lines and tissue specimens

MHCC97L cells were provided by the Liver Cancer Institute of Zhongshan Hospital, Fudan University (Shanghai, China). Huh7 and HEK293T cells were acquired from the American Type Culture Collection (ATCC, Manassas, VA, USA). Authentication of ATCC cell lines was performed using the GenePrint10 System (Promega Biotech Co.). The immortalized liver cell line LO2 and HCC cell line SMMC7721 was obtained from the cell bank of the Institute of Biochemistry and Cell Biology of the Chinese Academy of Sciences (Shanghai, China). Mouse LPC-Akt cells have been previously described [27]. All cell lines were authenticated by the examining of morphology and growth rate. Cell lines were maintained at 37 °C in 5% CO_2 in Dulbecco's modified Eagle medium (DMEM) supplemented with 10% fetal bovine serum. Cell lines were tested routinely for mycoplasma before use and all cell lines were used within 30 passages. A set of tissue microarrays (TMA) containing 78 HCC and non-tumoral tissue pairs were used for IHC staining. The basic clinicopathologic data were listed in Table S1. This study has been approved by the Ethics Committee of Renji Hospital, Shanghai Jiao Tong University School of Medicine. Liver tissues from *poh1*^{wt} or *poh1*$^{f/f}$, Mx-Cre^{+} mice were obtained as previously described [27]. In brief, the *poh1*$^{f/f}$ conditional knock-out mouse model (*poh1*$^{f/f}$) was created by Beijing Biocytogen. By crossing Mx-Cre mice with *poh1*$^{f/f}$ mice and then backcrossing, the generated *poh1*$^{f/f}$, Mx-Cre^{+} mice (6–8 weeks) were injected with three rounds of 5 μg/g body weight of poly I:C to induce *poh1* deletion in liver tissues. All animal experiments were subject to approval by the Animal Care Committee of Shanghai Jiaotong University.

2.3. Reagents and antibodies

Recombinant Human TGF-β1 Protein (240-B) was from R&D systems. Lipofectamine® 2000 or Lipofectamine® 3000 Transfection Reagent was from Invitrogen. Bafilomycin A1, Cycloheximide (CHX), puromycin, Thiazolyl Blue Tetrazolium Bromide (MTT, M5655) were from Sigma. MG132 (S2619) was from Selleck. TGFBR1 inhibitor LY-364947 (616451) was from Calbiochem. The primary antibodies used for western blotting were as follow: POH1 (CST, 4197, 1:1000), p-SMAD3 (abcam, ab52903, 1:1000), p-SMAD2 (CST, 3108, 1:1000), SMAD3 (proteintech, 25494-1-AP, 1:1000), SMAD2 (proteintech, 12570-1-AP, 1:1000), GAPDH (Santa Cruz, sc-25778, 1:1000), Flag-tag

(Sigma Aldrich, f1804, 1:1000), TGFBR1 (Thermo Fisher, PA5-14959, 1:500), TGFBR1 (Proteintech, 55391-1-AP, 1:500), TGFBR1 (Goat anti-TGFBR1, R&D, AF3025-SP), TGFBR2 (Themo Fisher, PA5-35076, 1:500), β-actin (Santa Cruz, sc-47778, 1:1000), HA-tag (Sigma Aldrich, H9658, 1:1000), V5-tag (Mouse anti-V5, MBL, M167-3, 1:1000), V5-tag (Rabbit anti-V5, CST, 13202S, 1:1000), CAV1 (proteintech, 16447-1-AP, 1:500) and ubiquitin (abcam, EPR8589, 1:1000). The primary antibodies used for immunohistochemistry were as follow: POH1 (Sigma, HPA002114), TGFBR1 (Thermo Fisher, PA5-14959, 1:100) and TGFBR2 (Themo Fisher, PA5-35076, 1:100).

2.4. Plasmids, siRNAs and cell transduction

Flag (3 × Flag)-tagged POH1(WT or ΔJAMM), V5-tagged TGFBR1 (WT), TGFBR1(T204D), TGFBR2(WT), POH1(WT), and CAV1(K-R) were cloned into pLVX plasmid. The plasmids expressing HA tagged wild-type ubiquitin (Addgene plasmid 17,608), K63-ubiquitin (Addgene plasmid 17,606) and K48-ubiquitin (Addgene plasmid 17,605) were kindly provided by Ted Dawson. HEK293t cells were used for lentivirus packaging. Lentiviral vectors expressing target genes were co-transfected with lentiviral packaging plasmids psPAX2 (Addgene plasmid, 12,260) and pMD2.G (Addgene plasmid, 12,259) with Lipofectamine® 3000 (Invitrogen). Viruses were harvested at 48 h and 72 h after transfection. Transduced cells were isolated by FASC sorting or puromycin selection.

The duplex siRNAs were chemically synthesized by Genepharma (Shanghai, China). The sequences of the siRNAs were as follows: POH1 si-1 (GGTCTTAGGACATGAACCA) and POH1 si-2 (GTGATTGATGTGTT TGCTA). siRNA transfection was performed using Lipofectamine® 2000 (Invitrogen) as standard protocol.

2.5. LC-MS/MS peptide identification

Proteins purified through immunoaffinity using Flag M2 Affinity Gel (Sigma, A2220) were resolved by SDS-PAGE followed by excised, digested with trypsin (Promega) into peptides and then subjected to LC-MS/MS (Liquid chromatography-tandem mass spectrometry) analysis.

LC-MS/MS identification of peptide mixtures was performed at Applied Protein Technology (aptbiotech, Inc. Shanghai, China). Briefly, peptides were chromatographed through the Easy-nLC 1000 system (Thermo Fisher). Peptide samples was loaded by Thermo Scientific Acclaim PepMap100 (100 μm*2 cm, nanoViper C18) and separated by Thermo scientific EASY column (10 cm, ID75μm, 3 μm, C18-A2) at 300 nL/min for 60 min using a three-step acetonitrile (0.1% formic acid in 84% acetonitrile) gradient: 0%–35% over the first 50 min and 35%–100% for 50-55 min and 100% for 55-60 min. The tandem mass spectrometry was performed by Q Exactive mass spectrometer (Thermo Fisher). The MS1 survey scan (300–1800 *m/z*) was at a resolution of 70,000 at 200 m/z with automatic gain control (AGC) target of 1e6 and a maximum injection time of 50 ms. Dynamic exclusion was 60.0 s. Each full scan take 20 MS2 scans. MS2 activation type was HCD model. Isolation window was 2 m/z. MS2 scan was at a resolution of 17,500 at 200 m/z with normalized collision energy 30 eV. Underfill was 0.1%. RAW files generated by spectrometer was subjected to Biopharma Finder1.0 software for protein identification. The search parameters were set as follows: Mass Values, Monoisotopic; Fixed modifications, Carbamidomethyl (C); Variable modifications, oxidation (M); Max modification/peptide, 2; Mass Accuracy, 10 ppm; Minimum confidence, 0.8. The data has been deposited to MassIVE Repository with the dataset identifier MSV000083366.

2.6. Pull down of cell surface receptors

Cells were washed with ice-cold PBS (supplemented with 0.9 mM $CaCl_2$ and 0.5 mM $MgCl_2$), then incubated with 0.5 mg/ml sulfo-NHS-SS-biotin (Thermo Fisher Scientific, 21,441) dissolved in PBS for 30 min at 4 °C. After the unreacted biotin was removed through 50 mM glycine, the cells were lysed by RIPA buffer. Biotinylated proteins were precipitated with Pierce™ High Capacity NeutrAvidin™ Agarose (Thermo Fisher Scientific, 29,202). Following three times washing with PBS, the indicated receptors were detected by immunoblotting.

2.7. In vivo pulmonary metastasis model

The *in vivo* lung metastasis models were established by MHCC97L and LPC-AKT cells. MHCC97L cells expressing the control vector or POH1 (3×10^6 cells per mouse) suspended by 0.2 ml PBS were injected *via* tail veins into the nude mice (5–6 weeks of age). After 50 days, the mice were sacrificed. LPC-AKT cells expressing the vector or POH1 (1×10^5 cells per mouse) in 0.2 ml PBS were injected through tail veins to the C57BL/6 mice (5–6 weeks age). The lungs were fixed with 4% paraformaldehyde and then subjected to Paraffin embedding and sectioning or fixed with Bouin's solution (Wuhan Goodbio Technology, Wuhan China) for observation. The paraffin sections were H&E stained, visualized and imaged with microscope. To evaluate seeding of tumor cells in the lung.

2.8. In vivo deubiquitination assay

HA-ubiquitinated TGFBR1-V5 or TGFBR2-V5 proteins were immunoprecipited using the anti-V5 antibodies in denaturing conditions. The target proteins were immune-purified with protein G agarose (Millipore, 16–266) and immunoblotted with antibodies against HA or ubiquitin.

2.9. In vitro deubiquitination assay

UB-HA conjugated TGFBR1(T204D)-V5 was purified from HEK293T cells by protein G-agarose (16–266, Millipore), then incubated with anti-V5 antibody. 3 × Flag tagged POH1(wild type or ΔJAMM form) was purified by anti-Flag M2 Affinity Gel (Sigma), and then incubated with 3 × Flag peptides (Sigma) to elute from the gel. HA-UB-TGFBR1 (T204D)-V5 and POH1 were incubated for 1 h at 37 °C in reaction buffer (50 mM Tris PH7.5, 10 mM MgCl2, 1 mM DTT, 100 mM NaCl, 1 mM ATP). The agarose was boiled with loading buffer and subjected to immunoblotted with antibodies against HA.

2.10. Transwell and wound healing assays

Cellular mobility was examined by transwell migration assays, that performed by Boyden chambers (8 μm-pore, Millipore, MA, USA) in 24-well plates. For invasion assays, the chambers were pre-coated by 50 μl Matrigel (BD Biosciences, MA, USA) and dried before use. 1×10^5 cells suspended by serum-free DMEM were seeded in the upper chambers, while the lower chambers were containing DMEM supplemented with 20% fetal bovine serum. Factors and inhibitors were added into upper and lower chambers. After incubation for 24 or 48 h at 37 °C in a CO2 incubator, the inserts were washed twice by PBS. The cells on the top surface of the chambers were wiped out by cotton swabs. The cells on the bottom surface of the cambers were then fixed by methanol, then stained by crystal violet and inspected using microscope. For the wound healing assays, cells were grown to confluence in the 6-well plates. Then the wounds were made by pipette tips. TGF-β (5 ng/ml) was used to treat cells 24 h before wounding and lasted to day 1 after that. The imaging was performed through a Phase-contrast microscope (Nikon, Shanghai, China).

2.11. Real-time PCR

To perform quantitative real-time RT-PCR, total RNA from cells were extracted through RNAiso Plus kit (Takara Bio Inc.). The cDNA

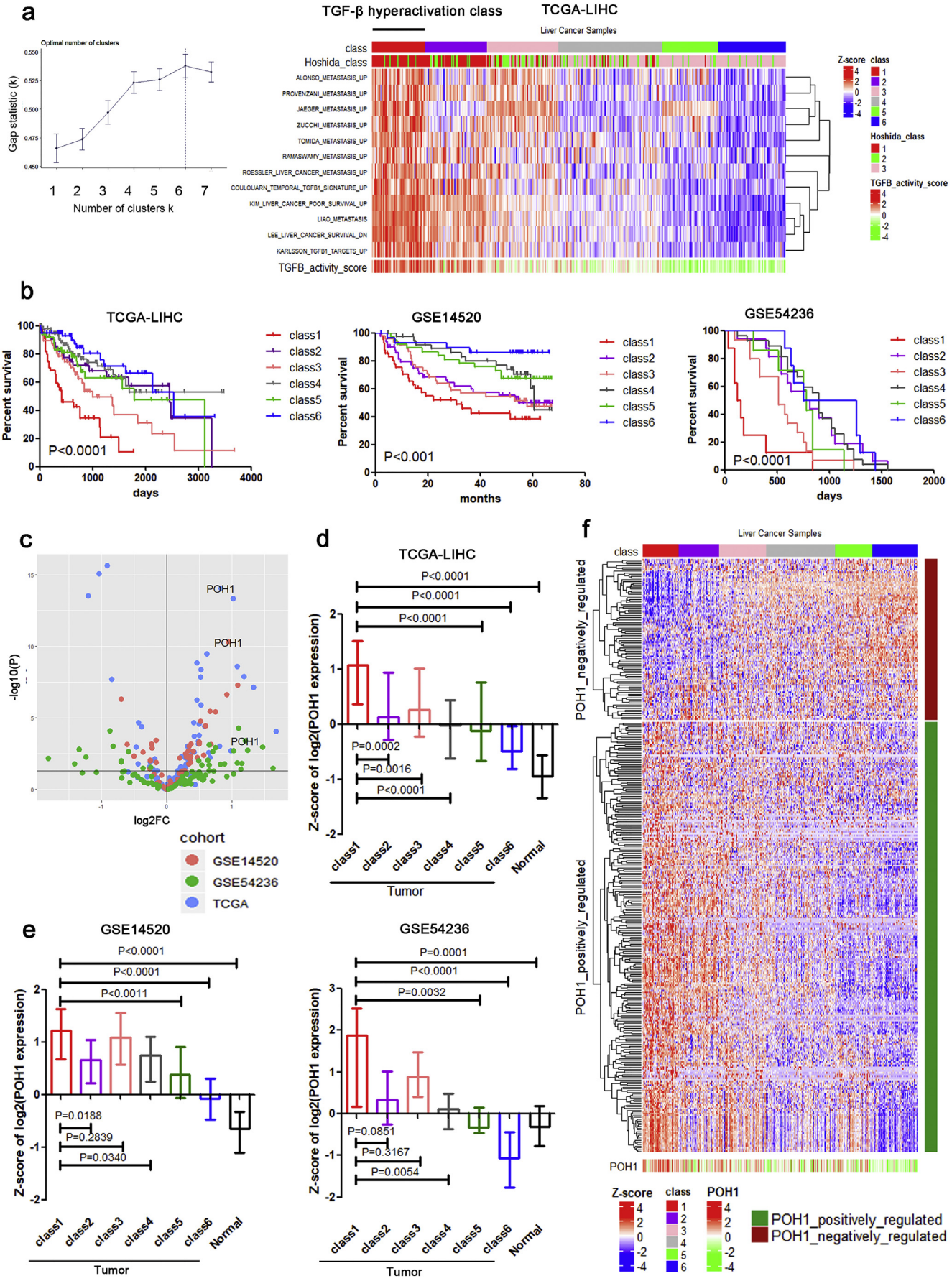
a
TGF-β hyperactivation class
TCGA-LIHC
Liver Cancer Samples
Optimal number of clusters
Gap statistic (k)
Number of clusters k
class
Hoshida_class
ALONSO_METASTASIS_UP
PROVENZANI_METASTASIS_UP
JAEGER_METASTASIS_UP
ZUCCHI_METASTASIS_UP
TOMIDA_METASTASIS_UP
RAMASWAMY_METASTASIS_UP
ROESSLER_LIVER_CANCER_METASTASIS_UP
COULOUARN_TEMPORAL_TGFB1_SIGNATURE_UP
KIM_LIVER_CANCER_POOR_SURVIVAL_UP
LIAO_METASTASIS
LEE_LIVER_CANCER_SURVIVAL_DN
KARLSSON_TGFB1_TARGETS_UP
TGFB_activity_score
Z-score
b
TCGA-LIHC
GSE14520
GSE54236
Percent survival
days
months
P<0.0001
P<0.001
class1
class2
class3
class4
class5
class6
c
POH1
-log10(P)
log2FC
cohort
GSE14520
GSE54236
TCGA
d
TCGA-LIHC
Z-score of log2(POH1 expression)
P<0.0001
P=0.0002
P=0.0016
Tumor
Normal
e
GSE14520
GSE54236
P<0.0011
P=0.0188
P=0.2839
P=0.0340
P=0.0032
P=0.0851
P=0.3167
P=0.0054
f
Liver Cancer Samples
POH1_negatively_regulated
POH1_positively_regulated
POH1
Z-score
class
POH1_positively_regulated
POH1_negatively_regulated

preparation was achieved based on standard procedures using primeScript RT Master kit (Takara Bio Inc.). Real-time PCR was performed by SYBR gGreen quantitative PCR kit (Life Technology) using the 7500 Real Time PCR System or ViiA7 System (AB Applied Biosystems). The primers used in the mRNA levels detection were as follows: human GAPDH-F: CATGAGAAGTATGACAACAGCCT, human GAPDH-R: AGTCCTTCCACGATACCAAAGT; TGFBR1-F: AAGAACGTTCG TGGTTCCGT, TGFBR1-R: CACCAACCAGAGCTGAGTCC; TGFBR2-F: GCAC GTTCAGAAGTCGGATG; TGFBR2-R: CTGCACCGTTGTTGTCAGTG, human CAV1-F: CGCGACCCTAAACACCTCAA; human CAV1-R: TCGTCACAGTG AAGGTGGTG.

2.12. Western blot

Cells or tissues were lysed by RIPA buffer (Thermo Fisher Scientific, 89,901) with protease inhibitors cocktail (Roche Diagnostics, 05892970001) and phosphatase inhibitor cocktail (Roche Diagnostics, 04906845001). The lysates were clarified by centrifugation at 13000*g* for 30 min at 4 °C. Protein concentrations were determined by BCA protein assay kit (Thermo Fisher Scientific, 23,225) followed by boiled with loading buffer. Protein samples (50–150 μg) were separated through SDS-PAGE, then transferred to NC membranes (Pall Corporation) blocked and incubated with the primary antibodies. After washing with TBST, the blots were incubated with goat anti-rabbit (Santa Cruz, sc-2004), goat anti-mouse (Santa Cruz, sc-2005) or mouse anti-goat (Santa Cruz, sc-2354) HRP (horseradish peroxidase)-conjugated secondary antibodies (Santa Cruz Biotechnology) and visualized using the SuperSignal West Dura Extended Duration Substrate (Thermo Fisher Scientific, 34,076).

2.13. Immunoprecipitation

Cells were harvested and lysed with an IP lysis buffer (Beyotime Institute of Biotechnology, P0013). Total protein (up to 5 mg) was incubated with Flag M2 Affinity Gel (Sigma, A2220) to immunoprecipitated the Flag-tagged proteins, overnight at 4 °C on a rocking platform. The immunoprecipitates were collected by centrifugation and washed three times with the cold TBS. the immunoprecipited protein complexes were eluted through 3 × Flag peptides (Sigma, F4799). The co-immunoprecipitated proteins were detected through western blot assay or subjected to the LC-MS/MS peptide identification.

Co-immunoprecipiation of the endogenous proteins was achieved by Protein G–agarose suspension (Millipore, 16–266). Total protein was incubated with 50 μl of Protein G–agarose suspension for 3 h at 4 °C on a rocking platform to reduce non-specific binding. After removing the beads, the supernatant was supplemented with the primary antibodies followed by incubation for an additional 3 h at 4 °C. A total of 100 μl of Protein G–agarose was then added to each immunoprecipitation mixture, and the incubation was continued overnight at 4 °C on a rocking platform. The immunoprecipitates were collected by centrifugation and washed three times with the TBS. The agarose was boiled with loading buffer and subjected to western blot analysis.

2.14. Immunohistochemistry

In the immunohistochemical staining assays, the slides were rehydrated and then immersed in 3% hydrogen peroxide solution for 15 min. Slides were pretreated by microwave for 25 min in 0.01 mol/L citrate buffer, pH 6.0, at 95 °C; and cooled naturally to room temperature. Between each incubation step, the slides were washed with PBS, pH 7.4. And then incubated overnight at 4 °C with diluted antibody against each protein studied. After washing with PBS, the sections were visualized using GTVisionTMIII Detection System/Mo&Rb (GeneTech, GK500710) as the manufacturer's instructions. IHC staining for POH1 and p-SMAD3 in human tissue samples was scored based on the intensity (1: low staining; 2: moderate staining; 3: high staining) and their percentage. The overall score the sum of intensity score × percentage.

2.15. Statistics

The correlation between protein expression levels was analyzed using the Spearman correlation test. The correlations between gene expression levels were calculated by Pearson correlation. Significant differences between groups were examined through student's *t*-test, Mann-Whitney test or Kruskal-Wallis rank sum test and Dunn's test of multiple comparisons. Kaplan–Meier survival analyses were tested by log-rank test. Factors that significantly impacted patient overall survival and progression-free survival were identified by both univariate and multivariate Cox proportional hazards regression models. The hazard ratios (HRs) and 95% confidence intervals were calculated. Statistical analyses were conducted by PASW 18.0 Statistical program (SPSS), GraphPad Prism 5 software and R statistical packages version 3.5.1. All *P* values <.05 were considered significant.

3. Results

3.1. HCC classification reveals a correlation between POH1 expression and poor prognosis

To categorize HCC patients into subclasses with respect to TGF-β signaling activity, metastasis potential and outcomes, we collected twelve signatures from Molecular Signatures Database (MSigDB) (Table S2) to cluster the patients from three independent cohorts. After calculating the Gap statistics to determine the optimal number of clusters, the TCGA-LIHC patients with scores of different signatures were clustered by k-means clustering algorithm into six classes (Fig. 1a). The overall scores of the signatures related to TGF-β signaling, high-metastatic and poor survival varied remarkably among the subgroups, showing a strong correlation between TGF-β activation and tumor progression. Notably, most patients in class1 group could be designated as Hoshida_class_C1 group, which represents a sub-population of HCCs with hyperactivated TGF-β signaling [10] (Fig. 1a, right). The rationality of the classification was then validated with other two GEO datasets (Fig. S1a). Furthermore, Kaplan Meier survival analyses were performed to test the differences of survival rates among different classes and confirmed that the patients from Class1 were worst in respect of overall survival in all three independent datasets (Fig. 1b). The genes that were statistically significant across all of the classes were determined by SAM-PAM algorithm and shown in Table S3.

Given the importance of deubiquitinating events in tumor progression, we set out to screen the differentially expressed DUBs between class1 and class 6 HCCs using three HCC databases. We found that POH1 was one of the DUBs displaying a significant upregulation in Class1 HCCs (Fig. 1c). Importantly, we observed remarkable

Fig. 1. Classification of HCC reveals a clinical significance of POH1 in malignant progression. (a) Unsupervised classification of patients in TCGA-LIHC cohort by k-means algorithm using ssGSEA scores of the TGF-β activity, metastasis and liver cancer survival related gene signatures. Left: Gap statistics analysis to determine the optimal number of clusters. Error bar = s.d. Right: Heatmap showing the subtypes classified by the activity scores of the signatures. Classification of the samples into Hoshida classes was performed by NTP analysis and showed in the heatmap, z-normalized by the rows. (b) Kaplan–Meier curves show the survival of HCC patients in the defined classes in TCGA-LIHC, GSE14520 and GSE54236 cohorts, *P* values were calculated by log-rank test and shown in the graph. (c) Volcano plots show the differences in DUB gene expression between class1 and class6 in TCGA-LIHC, GSE14520 and GSE54236 cohorts. (d-e) Comparison of POH1 expression between class1 with other classes by Kruskal-Wallis rank sum test and Dunn's test in TCGA-LIHC (d), GSE14520 and GSE54236 (e). The boxplots show the median with interquartile range. All Kruskal-Wallis test calculating *P* values <.0001, and the *P* values calculated by Dunn's multiple comparisons were shown in the graph. (f) Heatmap showing the expression levels of the POH1 positively and negatively regulated genes in the defined subpopulations, z-normalized by the rows.

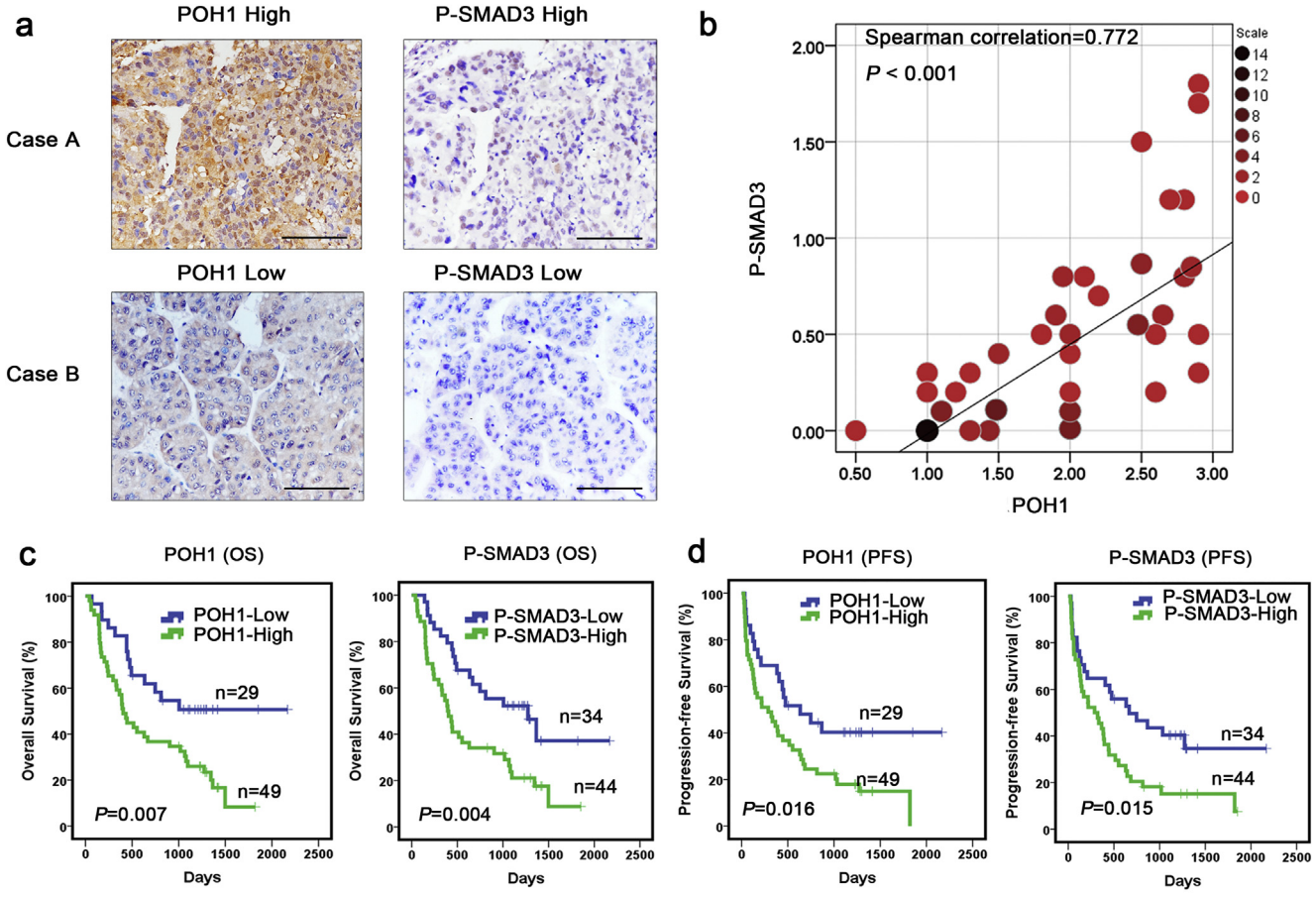

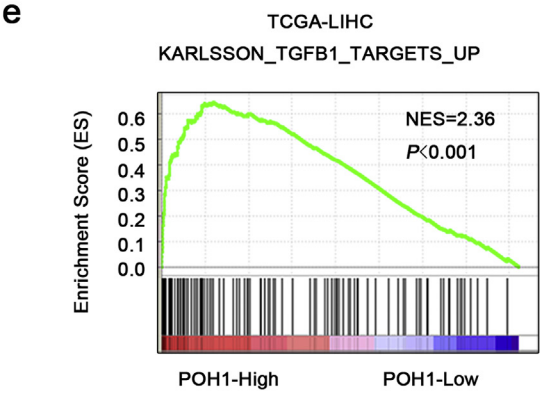

KARLSSON_TGFB1_TARGETS_UP

Dataset	NES	Normalized *P* value
TCGA-liver cancer	2.36	<0.001
GSE14520	2.06	<0.001
GSE25097	1.85	0.005870841
GSE39791	1.99	<0.001
GSE54236	2.22	<0.001
GSE57957	1.93	0.001956947
GSE62043	1.97	0.001934236
GSE76427	2.31	<0.001
GSE9843	1.95	<0.001

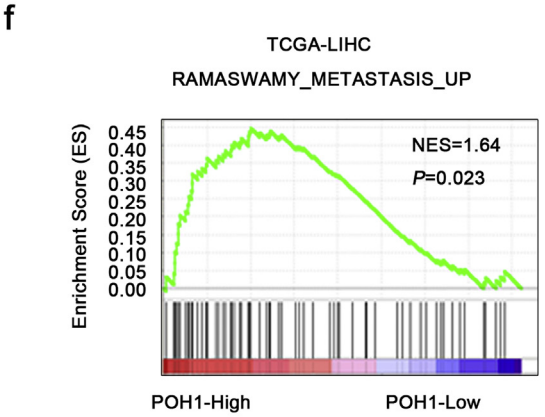

RAMASWAMY_METASTASIS_UP

Dataset	NES	Normalized *P* value
TCGA-liver cancer	1.64	0.023483366
GSE14520	2.00	0.001992032
GSE25097	1.65	0.02636535
GSE39791	1.7	0.017612524
GSE54236	1.63	0.019784173
GSE57957	1.42	0.11456311
GSE76427	1.66	0.021526419
GSE9843	1.75	0.011695907

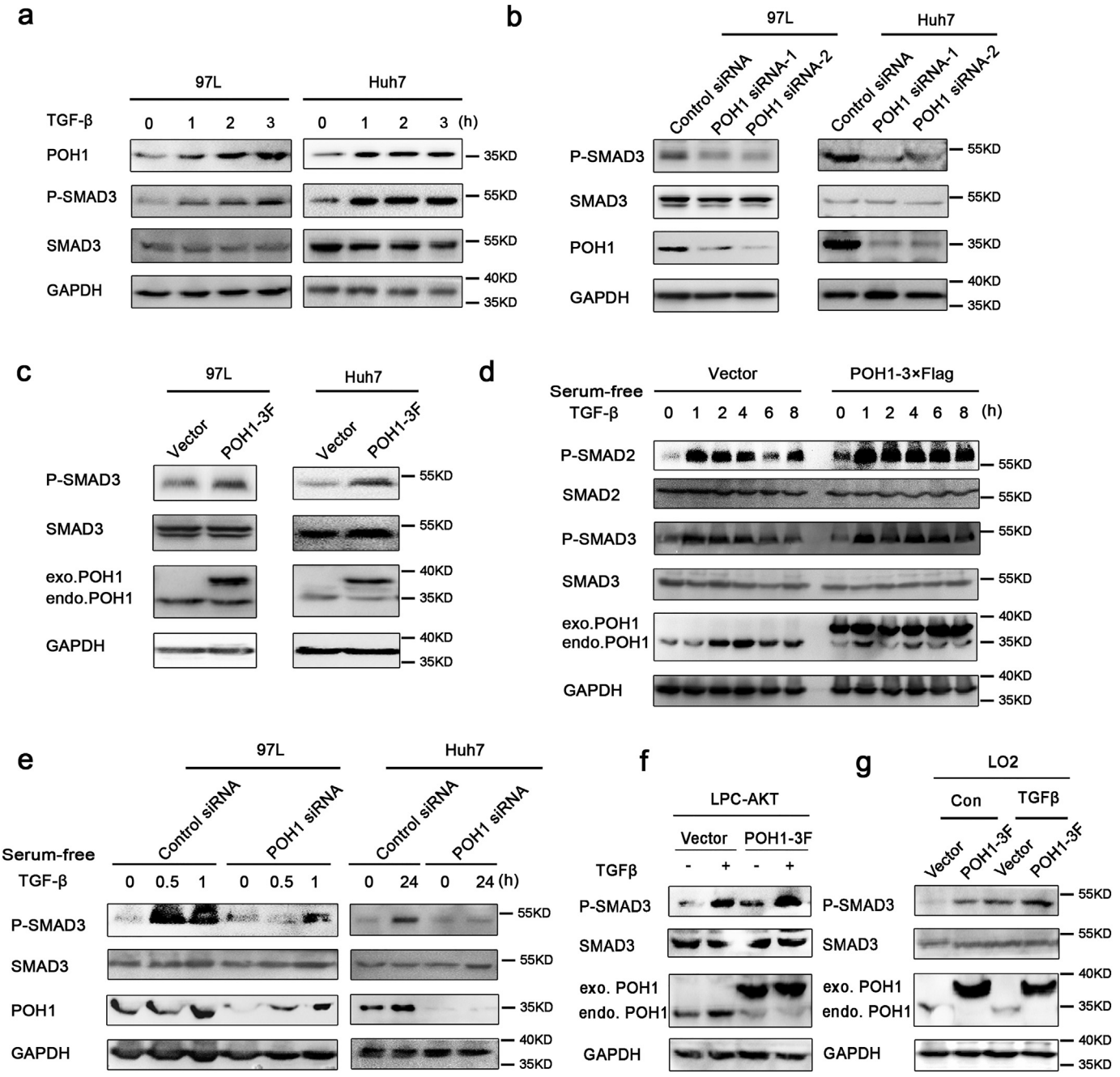

Fig. 3. POH1 enhances the activation of TGF-β signaling. (a) Immunoblot analyses of POH1 protein levels in the MHCC97L and Huh7 cells that were exposed to TGF-β (5 ng/ml) for the indicated time periods. (b) Immunoblot analyses of p-SMAD3 in HCC cells transfected with the indicated siRNAs. (c) Immunoblot analyses of p-SMAD3 in HCC cells with or without POH1–3 × Flag expression. (d) The MHCC97L cells stably expressing POH1–3 × Flag were deprived of serum overnight and then treated with TGF-β (5 ng/ml) for the indicated time periods. The cells were harvested and subjected to immunoblotting assays. (e) The MHCC97L and Huh7 cells transfected with POH1 siRNA were deprived of serum overnight and then treated with TGF-β (5 ng/ml) for the indicated time periods. The cells were harvested and subjected to immunoblotting assays. (f-g) Immunoblot analyses of p-SMAD3 levels in the LPC-AKT (f) and LO2 cells (g) stably expressing POH1–3 × Flag that were treated with TGF-β (5 ng/ml) for 4 h.

segregations among six groups in levels of POH1 expression, basically revealing a positive correlation between levels of POH1 transcripts and aggressiveness (Fig. 1d-e). Furthermore, assessing expression patterns of POH1 down-stream genes in the subgroups of HCCs showed that POH1 activity could be largely manifested by the classification (Fig. 1f). Correlation of POH1 expression with the reported molecular subclasses were also analyzed, and the results showed that a set of molecular signatures related to poorer prognosis or higher risk of

Fig. 2. POH1 expression positively correlates with TGF-β signaling. (a) Immunochemical analyses of POH1 and p-SMAD3 in 78 pairs of HCC tissues and the adjacent non-tumoral tissues. Representative specimens with high POH1 and p-SMAD3 staining (case A), low POH1 and p-SMAD3 staining (case B). (b) Correlation between POH1 and p-SMAD3 staining are shown, $P < .001$, by Spearman correlation test. (c-d) Kaplan–Meier curves show the overall survival (c) and progression-free survival (d) of HCC patients categorized with the scores of POH1 and p-SMAD3. All of the *P* values are shown in the graphs. (e-f) The gene set enrichment analyses were performed on liver cancer datasets from TCGA and GEO databases, based on POH1 expression levels, using a TGF-β positively regulated gene set (KARLSSON_TGFB1_TARGETS_UP) (e), and a metastasis-positively correlated gene set (RAMASWAY_METASTASIS_UP) (f). The representative GSEA results from each signature were shown in the left panels and the lists of the normalized enrichment score (NES) and *P* values in the indicated dataset were shown in right panels.

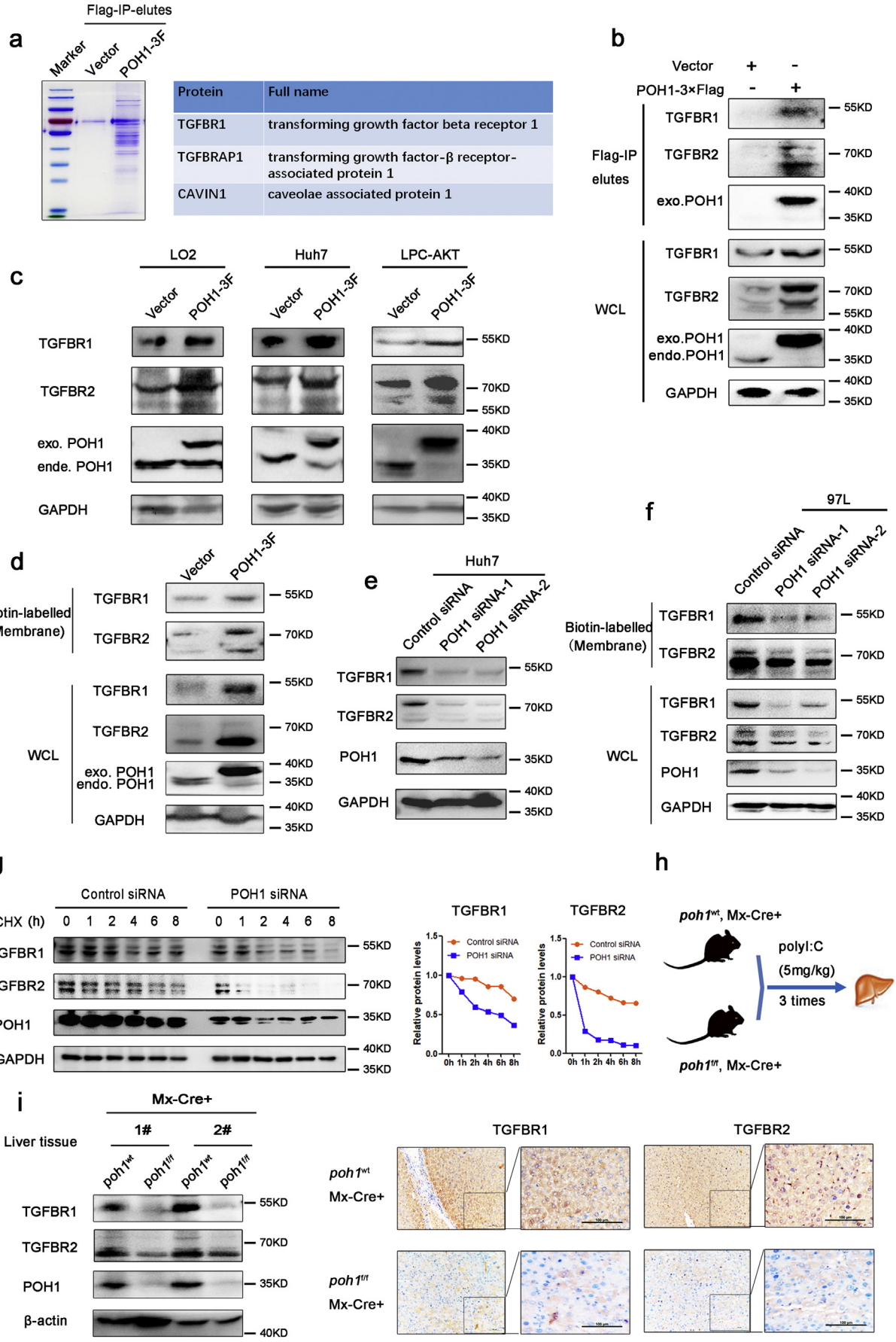
a
Flag-IP-elutes
Marker
Vector
POH1-3F
Protein
Full name
TGFBR1
transforming growth factor beta receptor 1
TGFBRAP1
transforming growth factor-β receptor-associated protein 1
CAVIN1
caveolae associated protein 1
b
Vector + -
POH1-3×Flag - +
Flag-IP elutes
TGFBR1
TGFBR2
exo.POH1
WCL
TGFBR1
TGFBR2
exo.POH1
endo.POH1
GAPDH
55KD
70KD
40KD
35KD
c
LO2
Huh7
LPC-AKT
Vector
POH1-3F
TGFBR1
TGFBR2
exo. POH1
ende. POH1
GAPDH
d
Vector
POH1-3F
Biotin-labelled (Membrane)
WCL
TGFBR1
TGFBR2
exo. POH1
endo. POH1
GAPDH
e
Huh7
Control siRNA
POH1 siRNA-1
POH1 siRNA-2
TGFBR1
TGFBR2
POH1
GAPDH
f
97L
Control siRNA
POH1 siRNA-1
POH1 siRNA-2
Biotin-labelled (Membrane)
WCL
TGFBR1
TGFBR2
POH1
GAPDH
g
Control siRNA
POH1 siRNA
CHX (h) 0 1 2 4 6 8 0 1 2 4 6 8
TGFBR1
TGFBR2
POH1
GAPDH
TGFBR1
TGFBR2
Control siRNA
POH1 siRNA
Relative protein levels
0h 1h 2h 4h 6h 8h
h
poh1wt, Mx-Cre+
polyI:C
(5mg/kg)
3 times
poh1f/f, Mx-Cre+
i
Mx-Cre+
Liver tissue
1#
2#
poh1wt
poh1f/f
TGFBR1
TGFBR2
POH1
β-actin
TGFBR1
TGFBR2
poh1wt
Mx-Cre+
poh1f/f
Mx-Cre+

recurrence were enriched in HCCs highly expressing POH1, whereas the signatures indicative of good outcome were enriched in the HCC population with low expression of POH1 (Fig. S1b). Collectively, our classification of HCC with different molecular signatures identifies POH1 as a DUB protein involved in regulating tumor progression.

We further explored the relationship between POH1 expression and survival rates using the information of the HCC databases. Indeed, high POH1 expression in tumors was significantly correlated with poor overall survival of HCC patients (Fig. S2a). Concurrently, gene set enrichment analyses of the TCGA and several GEO liver cancer datasets demonstrated a significant enrichment in the expression of a set of genes, which indicates poor survival of patients [32], in HCCs with high POH1 expression (Fig. S2b).

3.2. POH1 promotes TGF-β signaling in HCC cells

To further corroborate the clinical relevance of POH1 and TGF-β signaling in HCCs, we examined levels of p-SMAD3, an indicator of TGF-β activation, as well as the expression of POH1 in 78 pairs of HCC specimens and the adjacent non-tumoral tissues by immunohistochemical staining. Compared with non-tumoral liver tissues, both POH1 and p-SMAD3 scores were significantly elevated in HCC specimens (Fig. S2c). Importantly, we detected a positive correlation between POH1 and p-SMAD3 staining scores in these HCC samples ($P < .001$, by Spearman correlation test) (Fig. 2a-b). Collectively, these results strongly suggest that POH1 may promote TGF-β signaling in HCC.

Consistently, Kaplan-Meier analyses from the HCC samples revealed that the patients with higher staining scores of POH1 and p-SMAD3 had lower overall survival (Fig. 2c) and more advanced progression (Fig. 2d). Univariate Cox regression analyses showed that POH1 was significantly correlated with the risk of death and recurrence of HCC patients. In addition, the analyses with a multivariate Cox proportional hazards model indicated POH1 as an independent prognostic factor for both overall survival and progression-free survival in HCC patients (Table S4–5).

We further substantiated the clinical evidence linking the POH1 expression and TGF-β signaling in HCCs, and found that the TGF-β downstream signature (KARLSSON_TGFB1_TARGETS_UP) [33], which mirrors TGF-β activities, was significantly enriched in HCCs with high levels of POH1 in different cohorts (Fig. 2e). The positive correlation between levels of POH1 transcripts and scores of TGF-β activity in individual HCCs were exemplified with three databases (Fig. S2d). Of note, in addition to the correlation of POH1 expression with poor progression-free survival in HCC patients, the gene signature related to metastasis was found to be significantly enriched in the HCC specimens with high POH1 expression (Fig. 2f).

We next explored whether TGF-β regulates POH1 expression in cultured HCC cells. The results showed that TGF-β stimulation upregulated POH1 protein levels without influencing POH1 mRNA expression (Fig. 3a and Fig. S3a). These results promoted us to investigate whether POH1 is engaged in TGF-β signal transduction. Remarkably, we found that knockdown of POH1 substantially inhibited the basal levels of phosphorylated SMAD3 (Fig. 3b), whereas forced expression of POH1 yielded an opposite effect (Fig. 3c). Moreover, in the presence of exogenous TGF-β, hyper-activation of TGF-β signaling was greatly sustained by POH1 overexpression, as indicated by the phosphorylation of SMAD3 (p-SMAD3) and SMAD2 (p-SMAD2) (Fig. 3d and Fig. S3b). Importantly, when POH1 elevation by exogenous TGF-β was blocked by POH1 siRNA, the activation of TGF-β signaling was significantly suppressed (Fig. 3e). Similarly, overexpression of POH1 increased the levels of p-SMAD3 in $p53^{-/-}$, myristoylated AKT- transformed mouse liver progenitor cells (LPC-AKT) [27] (Fig. 3f), as well as the immortalized hepatocytes LO2 (Fig. 3g). Therefore, these results demonstrate a role for POH1 in promoting TGF-β activation in HCC.

3.3. POH1 interacts with and stabilizes TGF-β receptors

To understand how POH1 positively regulates TGF-β signaling, we performed high-throughput liquid chromatography-mass spectrometry (LC-MS/MS) analyses to identify the proteins potentially interacting with POH1. In brief, the protein complexes containing POH1-Flag were purified by anti-Flag antibody-conjugated resins, and the precipitated proteins eluted by 3 × Flag peptides were subjected to SDS-PAGE segregation and identification analyses (Fig. 4a, Fig. S3c and Table S6). Strikingly, in addition to a number of proteins known to interact with POH1, we identified TGFBR1 and several TGFBR1 partners as POH1-interacting protein candidates (Fig. 4a, right panel). This finding led us to hypothesize that increased TGF-β signaling by POH1 may be directly attributed to POH1 regulation of TGF-β receptor abundance. The interaction between exogenous and endogenous POH1 and TGFBR1 was further verified by co-immunoprecipitation assays (Fig. S3d-e). However, POH1 was not co-immunoprecipitated with SMAD7, a well-known negative regulator of the TGF-β receptor complex (Fig. S3f).

TGFBR1 is complexed with TGFBR2 to form heteromeric tetramers on cell surface, which initiates intercellular signal transduction [34]. We then examined the interaction of POH1 with the TGF-β receptor complexes *via* co-immunoprecipitation experiments and found that both TGFBR1 and TGFBR2 efficiently precipitated with POH1 (Fig. 4b). Consistent with these findings, expression of exogenous POH1 elevated both TGFBR1 and TGFBR2 in multiple cell lines (Fig. 4c and Fig. S3 g). The JAMM motif-depleted POH1 did not act as the wild-type POH1 to regulate the TGF-β receptors and TGF-β signaling activity (Fig. S3 h), indicating a requirement of deubiquitinase activity in this process. As expected, detection of biotinylated cell surface proteins revealed that POH1 increased the membrane-localized TGF-β receptors (Fig. 4d). Conversely, downregulation of POH1 by siRNAs decreased levels of TGFBR1 and TGFBR2 proteins in cells or on cell surface (Fig. 4e-f). Of note, the overexpression of POH1 did not result in a significant change in their mRNA levels (Fig. S3i), indicating that the POH1-mediated regulation of the TGF-β receptors involves post-transcriptional mechanisms. Accordingly, POH1 down-regulation efficiently decreased the stability of the TGF-β receptors (Fig. 4g). To evaluate whether POH1-mediated regulation of the TGF-β receptors occurs in primary mouse liver cells, we treated Mx-Cre^{+}, $poh1^{f/f}$ mice with poly I:C to induce POH1 depletion in liver cells (Fig. 4h) [27]. We found that ablation of POH1 in primary mouse liver tissues resulted in a significant reduction in levels of TGFBR1 and TGFBR2 proteins, as measured by western blotting and immunohistochemistry analyses (Fig. 4i and Fig. S3j).

Fig. 4. POH1 interacts with and stabilizes the TGF-β receptors. (a) Proteins immunoprecipitated with anti-Flag resins were resolved by SDS-PAGE and subjected to LC-MS/MS assays. Left: Coomassie brilliant blue staining of the PAGE gel. Right: TGFBR1 and the related proteins presented in the immunoprecipitates. (b) The MHCC97L cells transfected with POH1–3 × Flag were immunoprecipitated with Flag-M2 agarose beads. The eluates were immunoblotted to detect TGFBR1 and TGFBR2. (c) The LO2, Huh7 and LPC-AKT cells stably transfected with POH1–3 × Flag were subjected to immunoblotting assays using anti-TGFBR1 and TGFBR2 antibodies. (d) The MHCC97L cells stably transfected with POH1–3 × Flag were subjected to immunoblotting assays using anti-TGFBR1 and TGFBR2 antibodies. The biotinylated cell surface proteins were pulled down by neutravidin conjugated agarose and then detected by immunoblotting with anti-TGFBR1 and TGFBR2 antibodies. (e) Huh7 cells transfected with siRNAs were analyzed by immunoblotting through the indicated antibodies. (f) The MHCC97L cells transfected with siRNAs were analyzed by immunoblotting through the indicated antibodies. The biotinylated cell surface proteins were pulled down by neutravidin conjugated agarose and then detected by immunoblotting with anti-TGFBR1 and TGFBR2 antibodies. (g) Left: MHCC97L cells with or without POH1 siRNA transfection were treated with CHX (100 μg/ml) for the indicated time points. The cell lysates were analyzed by immunoblotting. Right: A plot of the normalized amounts of TGFBR1 and TGFBR2 proteins are shown. (h) Protocol of depleting *poh1* in liver tissues. (i) Left: Immunoblot analyses of TGFBR1 and TGFBR2 in liver tissues from $poh1^{wt}$, Mx-Cre^{+} and $poh1^{f/f}$, Mx-Cre^{+} mice treated with three rounds of poly I:C injections. Right: Immunohistochemical detection of TGFBR1 and TGFBR2 in liver tissues from the indicated groups. Representative images are presented. Scale bar = 100 μm.

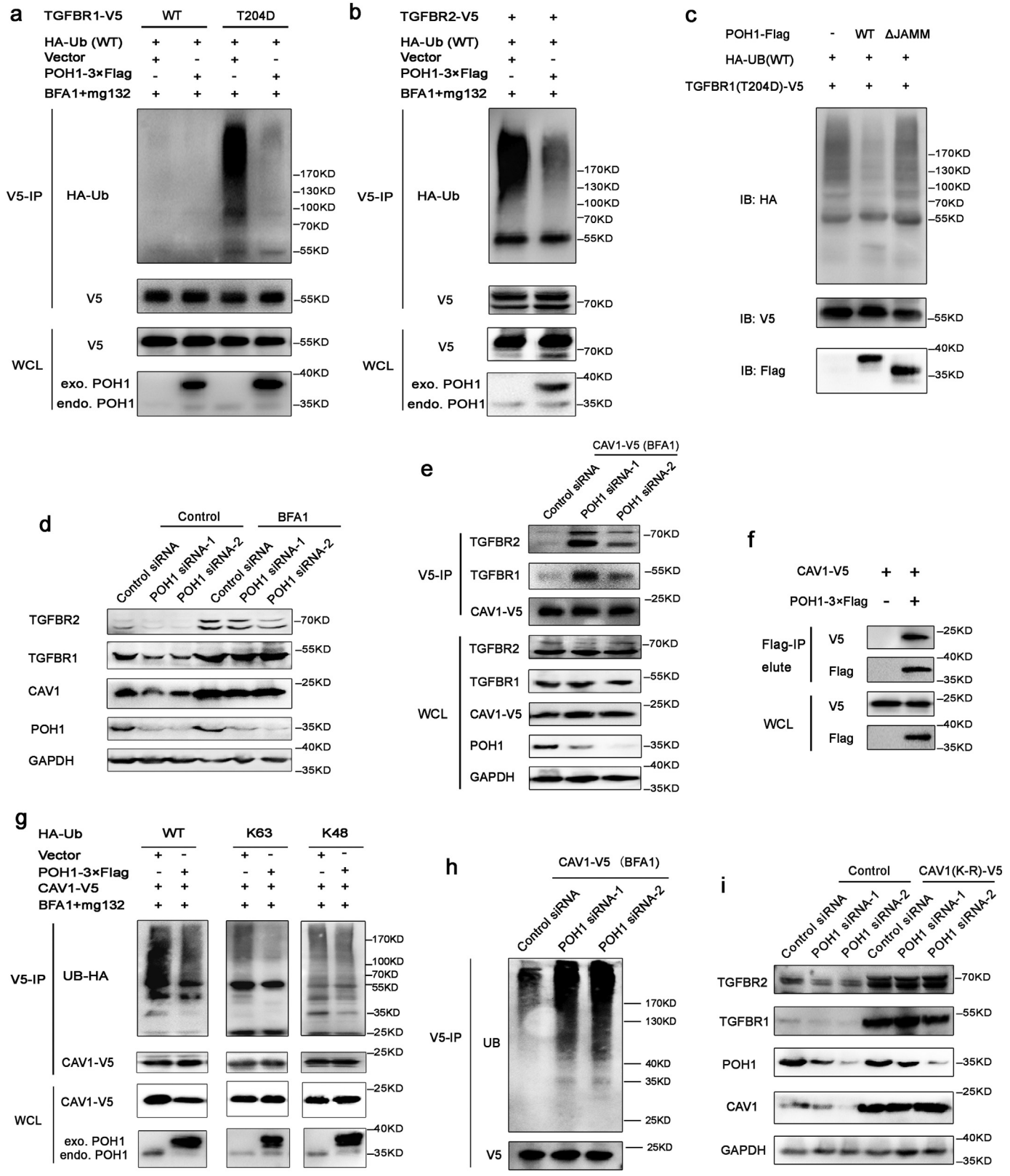

3.4. POH1 deubiquitinases the TGF-β receptors and caveolin-1

The turnover of the TGF-β receptors, both TGFBR1 and TGFBR2, is controlled by ubiquitination of these proteins, endocytosis and subsequent lysosomal degradation [35,36]. To determine whether the deubiquitinase POH1 attenuates the ubiquitination of TGFBR1 and TGFBR2. The deubiquitination assays showed that ectopically expressed POH1 dramatically decreased the levels of ubiquitinated TGFBR1 and TGFBR2 proteins (Fig. 5a-b). Moreover, we also found that both the K48 and K63 poly-ubiquitin chains of TGFBR1 and TGFBR2 proteins can be reduced in cells with POH1 overexpression (Fig. S4a-b). POH1 belongs to the JAMM domain metalloproteases and is specific for K63-linked polyubiquitin chains. The regulation of Ub-K48 chains of the

receptors by POH1 may be resulted from indirect mechanisms. To test this speculation, we performed *in vitro* deubiquitinating assays, the results showed that the wild-type POH1, efficiently removed Ub-WT, and —K63 chains, but not —K48 chains on the TGF-β receptors (Fig. 5c and Fig. S4c). In addition, while the treatment of the cells with lysosome inhibitor bafilomycin A1 (BFA1) rescued POH1 knockdown-mediated destabilization of the TGF-β receptors (Fig. 5d), the proteasome inhibitor Mg132 did not produce similar results (Fig. S4d), demonstrating the requirement of lysosomal activity in this process. It has long been appreciated that efficient trafficking of the TGF-β receptors to lysosomes is thought to be accomplished by caveolin-1 (CAV1)-coated lipid rafts, called caveolae, and CAV1 regulates TGF-β signaling *via* affecting the stability of TGF-β receptors [37,38]. Moreover, the polyubiquitination of CAV1 function as lysosomal trafficking signals to facilitate protein turnover [39–41]. The observations that loss of POH1 destabilized CAV1 protein (Fig. 5d and Fig. S4e-f) suggested an involvement of CAV1 in the POH1-mediated stabilization of the TGF-β receptors. Intriguingly, knockdown of POH1 increased the interaction between the TGF-β receptors and CAV1 (Fig. 5e), indicating that the endocytosis of these receptors by caveolae may be enhanced. We found that POH1 interacted with CAV1 (Fig. 5f), and substantially reduced wild type- and K63-linked ubiquitination on CAV1 proteins (Fig. 5g), and that knockdown of POH1 increased CAV1 polyubiquitination (Fig. 5h). We propose that downregulation of the ubiquitination of CAV1 by POH1 may lead to a downregulation of lysosomal degradation of the TGF-β receptors. We then generated a dominant-negative mutant form of CAV1, in which all 12 lysines were replaced by arginines (K-R) to eliminate their ubiquitination, and found that CAV1(K-R) expression dramatically increased levels of the TGF-β receptors and counteracted the POH1 knockdown-mediated down-regulation of the receptors (Fig. 5i). Collectively, these results suggest that POH1 can attenuate CAV1-mediated lysosomal degradation of TGFBR1 and TGFBR2 *via* deubiquitinating the TGF-β receptors and caveolin-1.

3.5. POH1 facilitates HCC cell metastasis through activating TGF-β signaling

The aforementioned clinical evidence indicate that POH1 is overexpressed in the aggressive subclass of HCC and correlates with metastatic signatures (Fig. 2f). We then examined whether POH1 promotes metastatic capabilities of liver tumor cells using *in vitro* and *in vivo* experiments. We found that POH1 knockdown significantly reduced the migration and invasion capability of HCC cells (Fig. 6a). While the exogenous expression of constitutively activated TGFBR1 (T204D) rescued the attenuated migratory ability (Fig. 6b), suggesting that POH1 regulates cellular metastatic potential *via* TGF-β signaling. In contrast, overexpression of POH1 significantly accelerated TGF-β-induced migration and invasion of HCC cells tested by transwell and wound healing assays (Fig. S5a-b), without altering the growth rate *in vitro* (Fig. S5c). Furthermore, these effects could be antagonized by the TGFBR1 inhibitor LY364947 (Fig. 6c and Fig. S5d).

We further examined the function of POH1 in promoting cancer cell metastasis. HCC cells with or without POH1 overexpression were injected into nude mice to generate experimental lung metastases. The results showed that overexpression of POH1 significantly promoted metastasis of MHCC97L HCC cells *in vivo* (Fig. S5e). Similar results were obtained in experiments using mouse liver LPC-AKT cells; POH1 overexpression significantly enhanced the formation of visible metastatic lung nodules (Fig. 6d).

Taken together, this study demonstrates that POH1 deubiquitinates the TGF-β receptors and CAV1 to attenuate lysosomal degradation of the receptors, thereby promoting TGF-β signaling and HCC metastasis (Fig. 6e).

4. Discussion

TGF-β signaling transduction initiates from the binding of TGF-β to the TGF-β receptor complex formed by TGFBR1 and TGFBR2 [34]. Deregulated function of the TGF-β receptors correlates with the metastatic potential of tumor cells and tumor aggression. Genetic or pharmaceutical disruption of TGF-β receptors alleviates the development and progression of liver cancer [5,6,42]. Our classification of HCCs with *in silico* data complements the previous finding that TGF-β signaling is critically contributive to HCC metastasis. Intrigued by the results of bioinformatics analyses and mass spectrometry, we performed a series of experiments in this study that demonstrate a functional interaction between POH1 and the TGF-β receptors and the clinical relevance of POH1-mediated stabilization of the TGF-β receptors in HCC.

The stability of TGF-β receptors is tightly regulated post-transcriptionally to ensure the appropriate onset of this signaling. TGF-β receptors modified with ubiquitination are usually targeted for lysosome-mediated degradation [35,36]. The TGF-β receptors undergo constitutive endocytosis by clathrin and CAV1-coated vehicles in the absence or presence of TGF-β [37]. Clathrin-positive vehicles are thought to contribute to TGF-β signaling activation [43], whereas caveolin-1-enriched lipid rafts can switch off the signaling by delivering the receptors to lysosomes for destruction [37,38]. Notably, several regulators can downregulate TGF-β signaling through caveolin-dependent degradation of the TGF-β receptors [44,45].

While regulation of TGF-β receptors by deubiquitination is important for proper TGF-β signaling in physiological scenarios, dysregulated expression of the DUBs that target TGF-β receptors are also implicated in various pathological processes [18,19,46]. The deubiquitinating enzyme POH1 has several substrates that function as pro-tumorigenic factors, including E2F1 [27], c-Jun [47], Mitf [48], Snail [28] and the cell surface protein Erbb2 [49]. Our study demonstrates that high POH1 expression in HCC contributes to hyperactivation of TGF-β signaling *via* deubiquitinating TGF-β receptors. Moreover, the modification of CAV1 by the K63-linked polyubiquitin chains enhances lysosomal sorting and protein clearance [39,40]. POH1 can remove the K63-polyubiqutin chains attached to CAV1 and compromise its activity in the lysosomal degradation of the TGF-β receptors.

Regarding the functional consequences of POH1-mediated promotion of TGF-β signaling in HCC cells, we found that POH1 substantially increased the metastatic potential of HCC cells both *in vitro* and *in vivo*. More importantly, the findings that POH1 promotes TGF-β signaling can be further demonstrated with clinical data. We detected a coordinated upregulation of POH1 and phosphorylated SMAD3 in HCC tissue samples. Furthermore, by analyzing several online datasets that

Fig. 5. POH1 reverses polyubiquitination of the TGF-β receptors and CAV1. (a–b) HEK293T cells overexpressing TGFBR1(WT or T204D)-V5 (a) or TGFBR2(WT)-V5 (b), POH1–3 × Flag and HA-tagged wild type-ubiquitin were lysed in denaturing conditions for immunoprecipitation with anti-V5 antibody. The cells were treated with 1 μM bafilomycin A1 and 25 μM mg132 for 6 h before collection. The ubiquitination levels were detected *via* the anti-HA antibody. (c) HA-UB(WT) modified TGFBR1(T204D)-V5 were purified from HEK293T cells with anti-V5 antibodies, the cells were treated with 1 μM bafilomycin A1 and 25 μM mg132 for 6 h before collection. 3 × Flag tagged POH1(WT or ΔJAMM) were purified from HEK293T cells with anti-Flag M2 resin. The ubiquitinated TGFBR1(T204D)-V5 and POH1–3 × Flag proteins were incubated for 1 h, and then immunoblotted with the indicated antibodies. (d) MHCC97L cells were transfected with POH1 siRNAs for 48 h, followed by treatment with 0.2 μM Bafilomycin A1 (BFA1) for another 24 h. The cell lysates were analyzed by detecting TGF-β receptors and CAV1. (e) MHCC97L cells stably expressing CAV1-V5 transfected with POH1 siRNAs were treated with BFA1 and immunoprecipitated with an anti-V5 antibody, and the co-immunoprecipitated TGFBR1 and TGFBR2 were detected by immunoblotting. (f) HEK293T cells were co-transfected with POH1–3 × Flag and CAV1-V5, followed by immunoprecipitation through an anti-Flag M2 resin, and the immunocomplexes were analyzed by immunoblotting. (g) HEK293T cells overexpressing CAV1-V5, POH1-Flag and HA-tagged different forms of ubiquitin. The cells were treated with 1 μM bafilomycin A1 and 25 μM mg132 for 6 h before collection. Cell lysates were immunoprecipitated with anti-V5 antibody, and the ubiquitination levels were analyzed by immunoblotting. (h) MHCC97L cells expressing CAV1-V5 were transfected with control or POH1 siRNAs, and CAV1-V5 proteins were immunoprecipitated with an anti-V5 antibody and analyzed by immunoblotting to detect ubiquitination levels. (i) MHCC97L cells expressing vector or CAV1(K-R)-V5 were transfected with POH1 siRNAs. The cell lysates were analyzed by detecting TGF-β receptors.

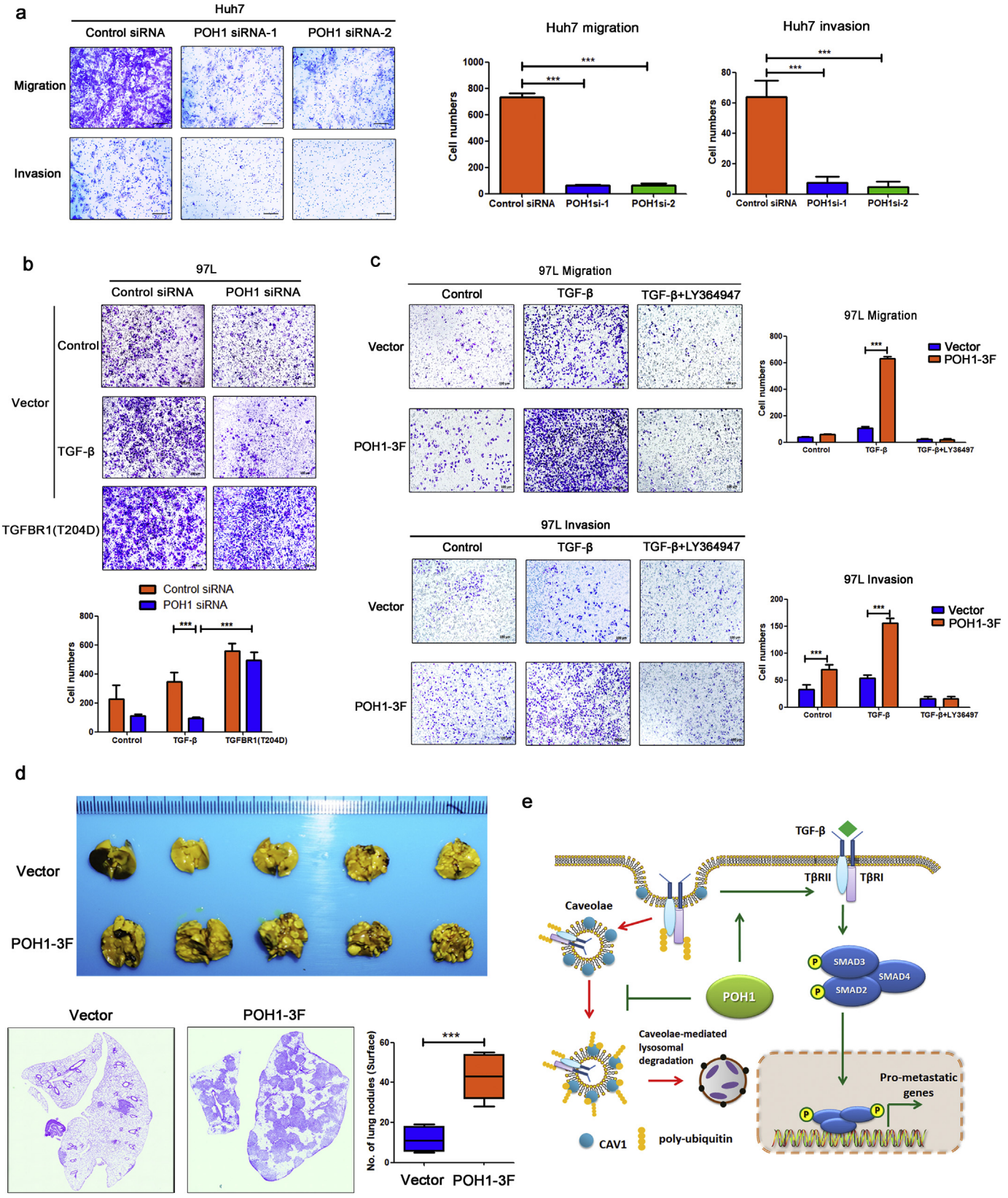

Fig. 6. POH1 promotes migration and invasion of HCC cells *via* TGF-β signaling. (a) Transwell assays show the effect of POH1 knockdown on the migration and invasion of Huh7 cells. Bar = 100 μm. Data shown are mean ± s.d. of 5 fields, $^{***}P < .001$ calculated by *t*-test. (b) Each group of MHCC97L cells was transfected with control or POH1 siRNA for 48 h, then subjected to transwell assays. Data shown are mean ± s.d. of 5 fields, $^{***}P < .001$ calculated by *t*-test. (c) Transwell assays show the effect of POH1 overexpression on cellular migration and invasion of MHCC97L cells with or without treatment of TGF-β (5 ng/ml) or TGF-β combined with LY364947 (10 μM). Quantification of the migrated cells and invaded cells were shown. Quantification of the metastatic cells was shown. Data shown are mean ± s.d. of 5 fields, $^{***}P < .001$ calculated by *t*-test. (d) LPC-AKT cells were injected into C57 mice through the tail vein. The mice were sacrificed 30 days later. The metastatic lung nodules on the surface of lungs and the representative images of the metastatic lung nodules were shown. The metastatic lung nodules were quantified and statistically analyzed by *t*-test. Data shown are mean ± s.d., $^{***}P < .001$, $n = 5$. (e) A schematic diagram for the proposed mechanism underlying POH1-mediated regulation of TGF-β signaling and HCC metastasis.

include different cohorts of HCC patients, we found that POH1 expression in HCC tissues was positively correlated with TGF-β signaling activity. In addition, our experiments and the data mining of multi-central datasets showed that HCC patients with high expression of POH1 exhibited low overall survival rates and were more likely to have recurrence, reinforcing a pathological significance for POH1 regulation of TGF-β signaling. Collectively, our study reveals an unappreciated role of POH1 in the regulation of the turn-over of the TGF-β receptors and demonstrates the contribution of the regulation to metastatic progression of HCC.

Funding sources

This work was supported by the National Natural Science Foundation of China (81672359, 81572293, 31770976, 81572694), the State Key Laboratory of Oncogenes and Related Genes (91-1705, 91-17-11), Shanghai Rising-Star Program (17QA1403700), Shanghai Sailing Program (18YF1421900), the grants from Shanghai Municipal Commission of Health and Family Planning (2017YQ040), and Shanghai Jiao Tong University School of Medicine (YG2017MS51).

Declaration of interests

The authors declare no conflict of interest.

Author contributions

B.W. and Y.Z.L. designed the research, analyzed data and wrote the manuscript; B.W., X.X., Z.Y., L.Z., Y.L., A.M., G.X., M.T., T.J., L.W. performed the experiments.

Appendix A. Supplementary data

Supplementary data to this article can be found online at https://doi.org/10.1016/j.ebiom.2019.01.058.

References

[1] Seoane J, Gomis RR. TGF-beta family signaling in tumor suppression and cancer progression. Cold Spring Harb Perspect Biol 2017;9(12).
[2] David CJ, Massague J. Contextual determinants of TGFbeta action in development, immunity and cancer. Nat Rev Mol Cell Biol 2018;19(7):419–35.
[3] Fabregat I, Moreno-Caceres J, Sanchez A, et al. TGF-beta signalling and liver disease. FEBS J 2016;283(12):2219–32.
[4] Wu K, Ding J, Chen C, et al. Hepatic transforming growth factor beta gives rise to tumor-initiating cells and promotes liver cancer development. Hepatology 2012;56(6):2255–67.
[5] Morris SM, Baek JY, Koszarek A, et al. Transforming growth factor-beta signaling promotes hepatocarcinogenesis induced by p53 loss. Hepatology 2012;55(1):121–31.
[6] Moon H, Ju HL, Chung SI, et al. Transforming growth factor-beta promotes liver tumorigenesis in mice via up-regulation of snail. Gastroenterology 2017;153(5):1378–91 [e6].
[7] Peng L, Yuan XQ, Zhang CY, et al. High TGF-beta1 expression predicts poor disease prognosis in hepatocellular carcinoma patients. Oncotarget 2017;8(21):34387–97.
[8] Sun H, Peng Z, Tang H, et al. Loss of KLF4 and consequential downregulation of Smad7 exacerbate oncogenic TGF-beta signaling in and promote progression of hepatocellular carcinoma. Oncogene 2017;36(21):2957–68.
[9] Coulouarn C, Factor VM, Thorgeirsson SS. Transforming growth factor-beta gene expression signature in mouse hepatocytes predicts clinical outcome in human cancer. Hepatology 2008;47(6):2059–67.
[10] Hoshida Y, Nijman SM, Kobayashi M, et al. Integrative transcriptome analysis reveals common molecular subclasses of human hepatocellular carcinoma. Cancer Res 2009;69(18):7385–92.
[11] Kumari N, Jaynes PW, Saei A, et al. The roles of ubiquitin modifying enzymes in neoplastic disease. Biochim Biophys Acta 2017;1868(2):456–83.
[12] Toloczko A, Guo F, Yuen HF, et al. Deubiquitinating enzyme USP9X suppresses tumor growth via LATS kinase and core components of the hippo pathway. Cancer Res 2017;77(18):4921–33.
[13] Alexopoulou Z, Lang J, Perrett RM, et al. Deubiquitinase Usp8 regulates alpha-synuclein clearance and modifies its toxicity in Lewy body disease. Proc Natl Acad Sci U S A 2016;113(32):E4688–97.
[14] Miotto B, Marchal C, Adelmant G, et al. Stabilization of the methyl-CpG binding protein ZBTB38 by the deubiquitinase USP9X limits the occurrence and toxicity of oxidative stress in human cells. Nucleic Acids Res 2018;46(9):4392–404.
[15] Ni Q, Chen J, Li X, et al. Expression of OTUB1 in hepatocellular carcinoma and its effects on HCC cell migration and invasion. Acta Biochim Biophys Sin 2017;49(8):680–8.
[16] Liu H, Chen W, Liang C, et al. WP1130 increases doxorubicin sensitivity in hepatocellular carcinoma cells through usp9x-dependent p53 degradation. Cancer Lett 2015;361(2):218–25.
[17] Xie X, Wang X, Liao W, et al. PPPDE1 promotes hepatocellular carcinoma development by negatively regulate p53 and apoptosis. Apoptosis 2018. https://doi.org/10.1007/s10495-018-1491-6 [Epub ahead of print].
[18] Zhang L, Zhou F, Drabsch Y, et al. USP4 is regulated by AKT phosphorylation and directly deubiquitylates TGF-beta type I receptor. Nat Cell Biol 2012;14(7):717–26.
[19] Eichhorn PJ, Rodon L, Gonzalez-Junca A, et al. USP15 stabilizes TGF-beta receptor I and promotes oncogenesis through the activation of TGF-beta signaling in glioblastoma. Nat Med 2012;18(3):429–35.
[20] Al-Salihi MA, Herhaus L, Macartney T, et al. USP11 augments TGFbeta signalling by deubiquitylating ALK5. Open Biol 2012;2(6):120063.
[21] Verma R, Aravind L, Oania R, et al. Role of Rpn11 metalloprotease in deubiquitination and degradation by the 26S proteasome. Science 2002;298(5593):611–5.
[22] Yao T, Cohen RE. A cryptic protease couples deubiquitination and degradation by the proteasome. Nature 2002;419(6905):403–7.
[23] Hao R, Nanduri P, Rao Y, et al. Proteasomes activate aggresome disassembly and clearance by producing unanchored ubiquitin chains. Mol Cell 2013;51(6):819–28.
[24] Butler LR, Densham RM, Jia J, et al. The proteasomal de-ubiquitinating enzyme POH1 promotes the double-strand DNA break response. EMBO J 2012;31(19):3918–34.
[25] Buckley SM, Aranda-Orgilles B, Strikoudis A, et al. Regulation of pluripotency and cellular reprogramming by the ubiquitin-proteasome system. Cell Stem Cell 2012;11(6):783–98.
[26] Byrne A, McLaren RP, Mason P, et al. Knockdown of human deubiquitinase PSMD14 induces cell cycle arrest and senescence. Exp Cell Res 2010;316(2):258–71.
[27] Wang B, Ma A, Zhang L, et al. POH1 deubiquitylates and stabilizes E2F1 to promote tumour formation. Nat Commun 2015;6:8704.
[28] Zhu R, Liu Y, Zhou H, et al. Deubiquitinating enzyme PSMD14 promotes tumor metastasis through stabilizing SNAIL in human esophageal squamous cell carcinoma. Cancer Lett 2018;418:125–34.
[29] Song Y, Li S, Ray A, et al. Blockade of deubiquitylating enzyme Rpn11 triggers apoptosis in multiple myeloma cells and overcomes bortezomib resistance. Oncogene 2017;36(40):5631–8.
[30] Luo G, Hu N, Xia X, et al. RPN11 deubiquitinase promotes proliferation and migration of breast cancer cells. Mol Med Rep 2017;16(1):331–8.
[31] Sadanandam A, Lyssiotis CA, Homicsko K, et al. A colorectal cancer classification system that associates cellular phenotype and responses to therapy. Nat Med 2013;19(5):619–25.
[32] Lee JS, Chu IS, Heo J, et al. Classification and prediction of survival in hepatocellular carcinoma by gene expression profiling. Hepatology 2004;40(3):667–76.
[33] Karlsson G, Liu Y, Larsson J, et al. Gene expression profiling demonstrates that TGF-beta1 signals exclusively through receptor complexes involving Alk5 and identifies targets of TGF-beta signaling. Physiol Genomics 2005;21(3):396–403.
[34] Zuniga JE, Groppe JC, Cui Y, et al. Assembly of TbetaRI:TbetaRII:TGFbeta ternary complex in vitro with receptor extracellular domains is cooperative and isoform-dependent. J Mol Biol 2005;354(5):1052–68.
[35] Xie F, Jin K, Shao L, et al. FAF1 phosphorylation by AKT accumulates TGF-beta type II receptor and drives breast cancer metastasis. Nat Commun 2017;8:15021.
[36] Meyer C, Liu Y, Dooley S. Caveolin and TGF-beta entanglements. J Cell Physiol 2013;228(11):2097–102.
[37] Di Guglielmo GM, Le Roy C, Goodfellow AF, et al. Distinct endocytic pathways regulate TGF-beta receptor signalling and turnover. Nat Cell Biol 2003;5(5):410–21.
[38] Chen YG. Endocytic regulation of TGF-beta signaling. Cell Res 2009;19(1):58–70.
[39] Sato M, Konuma R, Sato K, et al. Fertilization-induced K63-linked ubiquitylation mediates clearance of maternal membrane proteins. Development 2014;141(6):1324–31.
[40] Burana D, Yoshihara H, Tanno H, et al. The Ankrd13 family of ubiquitin-interacting motif-bearing proteins regulates valosin-containing protein/p97 protein-mediated lysosomal trafficking of caveolin 1. J Biol Chem 2016;291(12):6218–31.
[41] Hayer A, Stoeber M, Ritz D, et al. Caveolin-1 is ubiquitinated and targeted to intralumenal vesicles in endolysosomes for degradation. J Cell Biol 2010;191(3):615–29.
[42] Giannelli G, Villa E, Lahn M. Transforming growth factor-beta as a therapeutic target in hepatocellular carcinoma. Cancer Res 2014;74(7):1890–4.
[43] Mitchell H, Choudhury A, Pagano RE, et al. Ligand-dependent and -independent transforming growth factor-beta receptor recycling regulated by clathrin-mediated endocytosis and Rab11. Mol Biol Cell 2004;15(9):4166–78.
[44] Zhao B, Wang Q, Du J, et al. PICK1 promotes caveolin-dependent degradation of TGF-beta type I receptor. Cell Res 2012;22(10):1467–78.
[45] Chen CL, Yang PH, Kao YC, et al. Pentabromophenol suppresses TGF-beta signaling by accelerating degradation of type II TGF-beta receptors via caveolae-mediated endocytosis. Sci Rep 2017;7:43206.
[46] Liu S, de Boeck M, van Dam H, et al. Regulation of the TGF-beta pathway by deubiquitinases in cancer. Int J Biochem Cell Biol 2016;76:135–45.
[47] Nabhan JF, Ribeiro P. The 19 S proteasomal subunit POH1 contributes to the regulation of c-Jun ubiquitination, stability, and subcellular localization. J Biol Chem 2006;281(23):16099–107.
[48] Schwarz T, Sohn C, Kaiser B, et al. The 19S proteasomal lid subunit POH1 enhances the transcriptional activation by Mitf in osteoclasts. J Cell Biochem 2010;109(5):967–74.
[49] Liu H, Buus R, Clague MJ, et al. Regulation of ErbB2 receptor status by the proteasomal DUB POH1. PloS one 2009;4(5):e5544.